



Image Steganography Based on Wavelet Transform and Color Space Approach

Adel Jalal Yousif*

Electronic computer center, University of Diyala, 32001 Diyala, Iraq

ARTICLE INFO

Article history:

Received 8 August 2019
Accepted 10 June 2020

Keywords:

Image steganography; Discrete wavelet Transform (DWT); YCbCr color space; Singular value decomposition (SVD); Structural Similarity Index Measure (SSIM).

ABSTRACT

This paper presents a color image steganography scheme based on discrete wavelet transform (DWT) and YCbCr color space. The cover image is initially transformed from RGB color space into YCbCr and the Cb component is utilized for hiding a secret grayscale image. Two-level DWT is applied to the selected component to obtain the horizontal sub-band HL2 which is used for the embedding process based on the singular value decomposition (SVD) of the secret image and the obtained sub-band HL2 of the cover image. Structural Similarity Index Measure (SSIM) and Peak Signal to Noise Ratio (PSNR) are measured for evaluating the performance of the proposed scheme. Simulation results show that the proposed steganography method is reliable against several attacks without degrading the visual quality of the cover image. Further, comparative results for the proposed method in YCbCr and RGB color spaces show that the YCbCr space is more efficient in secret image retrieval.

1 Introduction

Due to the increased development in multimedia processing techniques and applications, it has become potential to manipulate a huge amount of multimedia sent over the internet or any other network. Internet access makes inserting, modifying, deleting and/or distributing digital content easier and cheaper. Thus, the process of transferring data over the internet may be insecure. To handle this issue, many techniques of data security have been proposed. The two most popular and related among them are cryptography and steganography, which are used essentially for protecting data against malicious activities or unwelcome parties [1]. The key difference between cryptography and steganography is preserving the presence of a message secret. In the case of cryptography, the message is changed in some way so that it is visible but cannot be understood by the unintended person.

Whereas, steganography hides the fact that the message exists by concealing it within another media. In other words, digital steganography can be defined as the process of concealing secret information within a data carrier in such a way that the presence of the secret information is unnoticeable. Therefore, steganography offers an extra layer of protection on the secret information compared with cryptography [2]. In general, the secret information can be extracted by applying the embedding algorithm inversely at the intended recipient.

Steganography systems are mainly characterized by three challenging factors: imperceptibility, robustness, and capacity. Imperceptibility of steganography refers to the ability to conceal information without being noticed by humans detects. While robustness measures the steganography resistance against signal manipulation or even external attacks without affecting the process of extracting

* Corresponding author.

E-mail address: adel.jalal@uodiyala.edu.iq

DOI: 10.24237/djes.2020.13303

hidden information. Robustness and imperceptibility are the most important factors in measuring the quality of the steganography techniques because they conflict each other, where increasing robustness means decreasing imperceptibility and vice versa so it is better to have some balance between them. Whereas, capacity affects both robustness and imperceptibility in the same manner, which indicates the amount of secret information that is concealed in the data carrier [3,4].

The image steganography techniques are mainly categorized into two approaches: spatial domain and frequency domain. In spatial-domain, the secret message is inserted within the cover image by altering the intensity of certain pixels, such as in the Least Significant Bit (LSB) method [5]. Whereas in the frequency domain, the cover image is firstly transformed into the frequency domain then the secret message is inserted within the cover image coefficients. The most commonly used transformations are Discrete Cosine Transform (DCT) [6] and Discrete Wavelet Transform (DWT) [7]. These transformational methods have more advantages compared to spatial domain methods where they are more secure and attacks tolerant as explained by several surveys [4,8,9,10]. So, the frequency domain is employed for the proposed method.

2 Discrete wavelet transform

The use of the Discrete Wavelet Transform (DWT) is growing rapidly because of its effectiveness in many different fields. By applying 2D-DWT, the input signal is firstly separated into two bands, low frequency and high frequency bands by performing low-pass (L) and high-pass (H) filters in a horizontal direction. Then, each of these bands is separated again into two sub-bands by performing the same filters but in a vertical direction resulting in four sub-bands which are denoted by approximation (LL), horizontal (HL), vertical (LH), and diagonal (HH). For this notation, the first character L or H indicates the type of filter low-pass (L) or high-pass (H) applied horizontally and the second one L or H indicates the same type of filter applied vertically as shown in Figure 1. The approximation (LL) sub-band represents a low-frequency component which consists of the most significant image features. Whereas, the other three sub-bands represents a high-frequency component which consists of the most significant image features. Whereas, the other three sub-bands represents a high-frequency component including image details. The human eye is less sensitive to change in the high-frequency component [11, 12]. So in this work, the horizontal sub-band HL is chosen for hiding the secret image to improve both robustness and perceptual quality simultaneously.

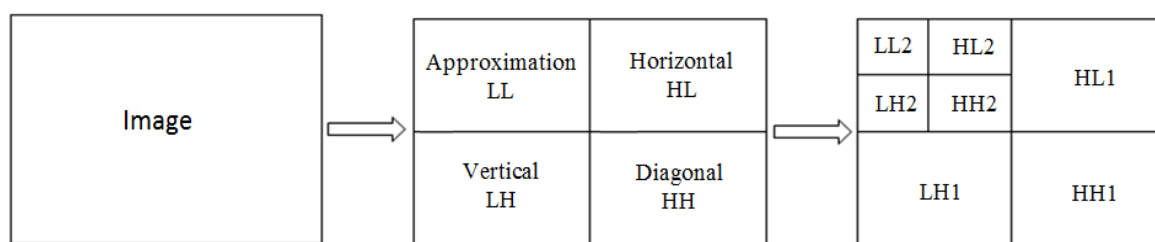


Fig. 1. Two level discrete wavelet decomposition

3 Singular value decomposition

SVD is one of the most significant numerical analysis techniques which can be utilized to factorize a matrix into three matrices based on linear algebra. SVD has been applied

efficiently in different signal processing fields such as noise reduction, data compression, pattern analysis, and image hiding due to its important mathematical properties such as high stability. For an image A of size $M \times N$, the SVD can be given by [13]:

$$A=U S V^T \quad (1)$$

where U and V are the orthogonal matrices with the size of $M \times M$ and $N \times N$ respectively, S is the diagonal or singular matrix with the size of $M \times N$ and the superscript T indicates the transposition of the matrix. The columns of U and V are known as left singular vectors and right singular vectors respectively and the elements of the S matrix is called singular values. The singular vectors of U and V represent the geometrical image property while the singular values of S represent the image luminance. The essential advantage of using SVD is that when the singular matrix is used in image steganography, a lesser number of values of the cover image are modified. Thus, when a small modification is made to an image, it does not change its visual perception significantly[14].

4. Color space

A color image generally consists of three basic components and can be represented by different mathematical models called color

spaces. One of the most widely used is RGB color space, but color components in RGB color space are highly correlated and each color component has redundant information with the other two components. This property of RGB color space is not preferred in some digital image applications such as image steganography and image segmentation. Therefore, another color space can be used such as YCbCr due to its high decorrelation color values as compared to RGB space as shown in Figure 2. In YCbCr, Y specifies light intensity or brightness, Cb and Cr specify color information. So, brightness and chroma are separated in YCbCr. In this work, the Cb component is utilized for secret image hiding because the human eye is less sensitive to change in blue color [15]. RGB to YCbCr transformation can be described as follows[16]:

$$Y = (0.257 R) + (0.504 G) + (0.098 \times B) + 16$$

$$Cb = (0.439 \times R) - (0.368 \times G) - (0.071 \times B) + 128 \quad (2)$$

$$Cr = (0.148 \times R) - (0.291 \times G) + (0.439 \times B) + 128$$



Fig. 2. Color image conversion from RGB to YCbCr space: (a) RGB image, (b) YCbCr image, (c) Y-component, (d) Cb-component, (e) Cr-component

5. Proposed work

The proposed steganography scheme is based on three transformation techniques (YCbCr space, DWT, and SVD). The secret information is encoded in the horizontal sub-band HL2 of the Cb component in YCbCr space by applying 2-level DWT and then SVD technique. The algorithms for secret image embedding and extraction are described below and illustrated in Figures 3 and 4 respectively.

5.1 Algorithm for embedding process

Step1: Read the cover image and the secret image which are denoted by h and s respectively.

Step2 : Obtain the Cb component of the original cover image by converting its color space from RGB to YCbCr by using Eq.2.

Step3: Perform 2 level 2D-DWT on the selected Cb component to obtain the horizontal sub-band HL2 as

$$[LL1, LH1, HL1, HH1] = DWT(Cb)$$

$$[LL2, LH2, HL2, HH2] = DWT(LL1)$$

Step 4: Decompose the obtained HL2 into three matrices by applying SVD technique:

$$[U_h S_h V_h] = SVD(HL2) .$$

Step5: Perform SVD technique to the secret image S :

$$[U_s S_s V_s] = SVD(S)$$

Step6: Modify the singular value of HL2 by using the singular value of secret image as:

$$S_{h'} = S_h + \alpha * S_s$$

where, $S_{h'}$ represents the singular value of the stego image, and α represents the embedding coefficient which is discussed in section 6.

Step7: Obtain the altered sub-band $HL_{h'}$ using SVD technique with the modified singular value as:

$$HL_{h'} = U_h S_{h'} V_h^T$$

Step8: Apply 2 level inverse 2D-DWT to get the modified Cb' component:

$$LL1_{h'} = IDWT [LL2, LH2, HL_{h'}, HH2]$$

$$Cb' = IDWT [LL1_{h'}, LH1, HL1, HH1]$$

Step9: Combine Y, Cb', and Cr components to obtain YCbCr image.

Step10: Convert the obtained image from YCbCr space to RGB to get the stego image (h').

5.2 Algorithm for extraction process

Step1: Read the stego RGB image (h')

Step2: Convert color space of the stego image from RGB into YCbCr to get Cb' component.

Step3: Perform 2 level 2D-DWT on Cb' component to obtain HL2 as:

$$[LL1, LH1, HL1, HH1] = DWT(Cb')$$

$$[LL2, LH2, HL2, HH2] = DWT(LL1)$$

Step4: Decompose the obtained HL2 by applying SVD technique:

$$[U_{h'} S_{h'} V_{h'}] = SVD (HL2).$$

Step5: Obtain the singular values of the secret image by: $S_e = (S_h - S_{h'}) / \alpha$.

Step6: Extract the secret image S' by applying SVD technique based on orthogonal matrices U_s and V_s as:

$$S' = U_s S_e V_s^T .$$

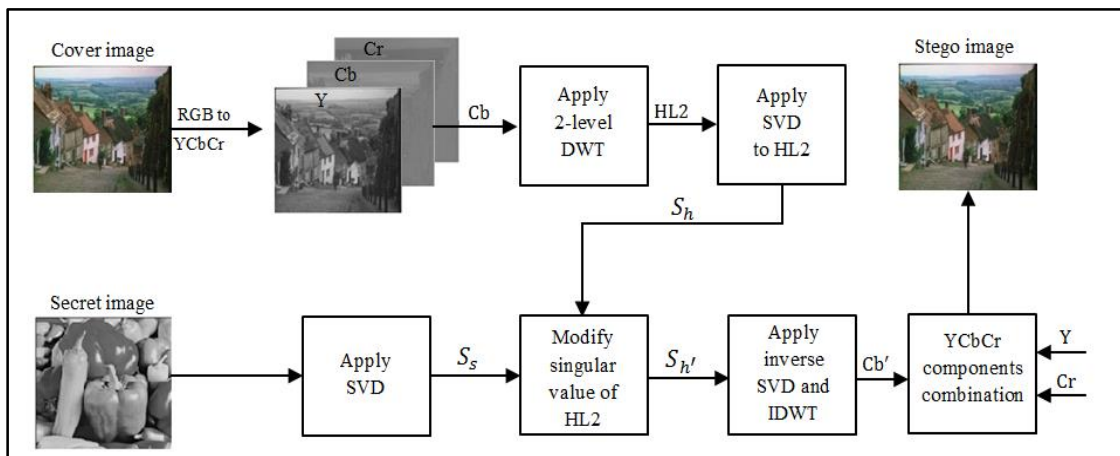


Fig.3. Secret image embedding algorithm

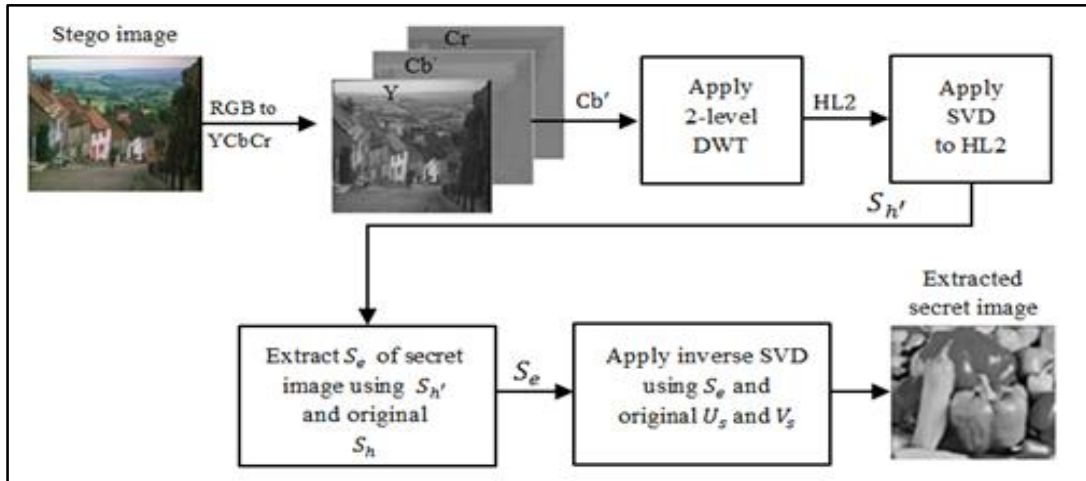


Fig. 4. Secret image extraction algorithm

6. Results and discussion

The performance of digital steganography techniques is typically evaluated by estimating firstly the robustness of the embedded secret image against common image processing operations of the stego image and secondly the secret image imperceptibility to human observers. The proposed algorithm is simulated with the MATLAB R2018a program by using three well-known 24-bit color images (Goldhill,

Airplane, and House) of size 512×512 as cover images for embedding an 8-bit grayscale image (peppers) of size 64×64 as a secret image as shown in Figure 5. For assessing the robustness of the proposed algorithm, Structural Similarity Index Measure (SSIM) is used to calculate the degree of similarity between the extracted secret image and the original one. SSIM can be considered as a perception-based model in which image distortion is represented by a perceived change in structural information

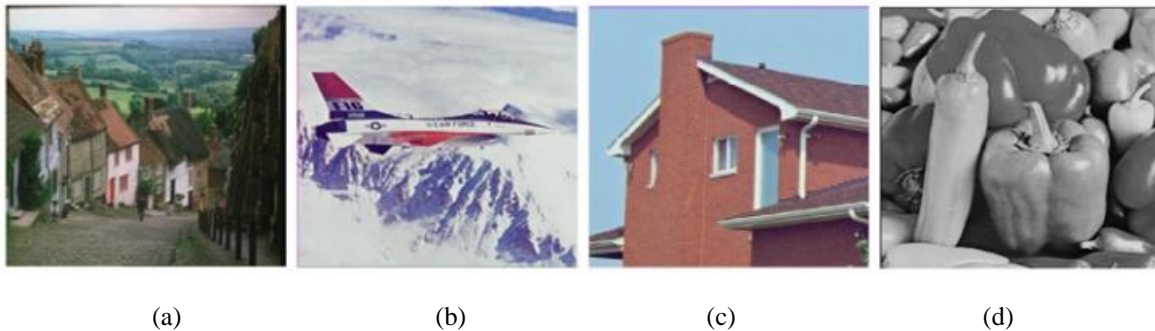


Fig. 5. Test images used for experiments: (a) Goldhill, (b) Airplane (c) House, (d) Peppers

Hence, it is possible to say that SSIM is correlated with the quality perception of the human visual system. An SSIM value is between -1 and 1; the larger the value is, the higher the similarity of the two images is. The equation of SSIM for two images x and y can be described as [17]:

$$SSIM(x, y) = f(l(x, y).c(x, y).s(x, y)) \quad (3)$$

where $l(x, y)$ is the luminance distortion component, $c(x, y)$ is the contrast distortion component, $s(x, y)$ is the structure variations component, and $f(\cdot)$ is the combination function. These three components are given as follows:

$$I(x, y) = \frac{2u_x 2u_y + C_1}{u_x^2 + u_y^2 + C_1}, C_1 = (K_1 L)^2 \quad (4)$$

$$c(x, y) = \frac{2\sigma_x 2\sigma_y + C_2}{\sigma_x^2 + \sigma_y^2 + C_2}, C_2 = (K_2 L)^2 \quad (5)$$

$$s(x, y) = \frac{2\sigma_{xy} + C_3}{\sigma_x \sigma_y + C_3}, C_3 = C_2 / 2 \quad (6)$$

where u_x and u_y represent the mean value of x and y respectively, L represents the dynamic range of pixel intensity ($L = 256$), $K_1 = 0.01$ and $K_2 = 0.03$. σ_x and σ_y are the standard deviations of x and y respectively, and σ_{xy} represents the correlation coefficient of x and y . To assess the imperceptibility of the secret image, the peak signal to noise ratio (PSNR) is utilized to calculate the stego image quality. A high value of PSNR ensures less degradation in stego image and more imperceptibility of steganography method. PSNR can be described by the following equation [18]:

$$PSNR = 10 \log_{10} \left(\frac{255^2}{MSE} \right) \quad (7)$$

where, MSE is the mean square error between original and stego image, the MSE is given by:

$$MSE = \frac{\sum_{x=1}^M \sum_{y=1}^N (h(x, y) - h'(x, y))^2}{M \times N} \quad (8)$$

The value of the embedding coefficient α mainly affects the performance of the proposed algorithm where a high value of α ensures a high level of robustness while degrades the stego image quality as shown visually in Figure 6 and arithmetically in table 1. Hence, the embedding coefficient value should be accurately chosen to achieve an acceptable tradeoff between imperceptibility and robustness. In this work, the suggested value of α is 0.1 based on experiments. Additionally, the value of α can be changed according to the cover image characteristics and the desired level of robustness.

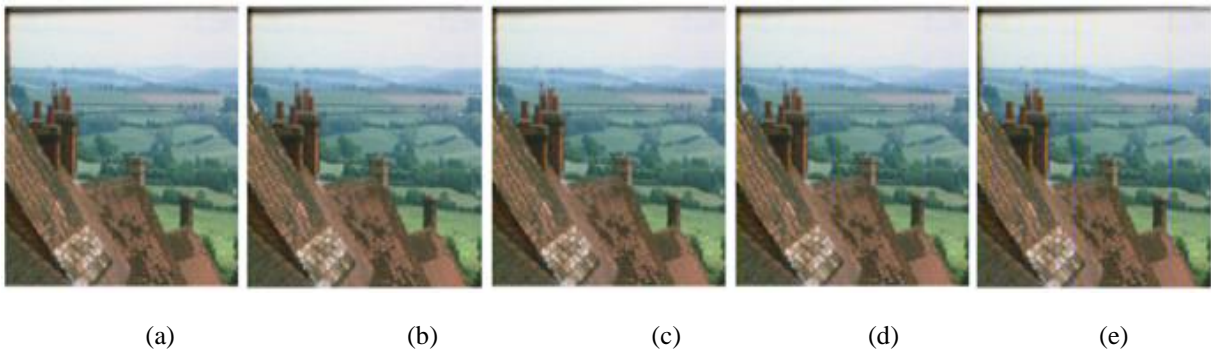


Fig. 6. Enlarged part of stego Goldhill image with different values of α : (a) Original, (b) $\alpha = 0.05$, PSNR = 46.36, (c) stego $\alpha = 0.1$, PSNR = 43.00, (d) stego $\alpha = 0.2$, PSNR = 39.36, (e) stego $\alpha = 0.4$, PSNR = 35.85

Figure 7 shows the results of the stego Goldhill image which is subjected to different known attacks with the corresponding extracted secret Peppers image. Performance analysis and comparison of the proposed technique with the steganography scheme in [19] is presented in

tables 2 in term of PSNR and SSIM, the tested images are exposed to various type of attacks including (image cropping, histogram equalization, median filtering, speckle noise, Gaussian noise, and salt & pepper noise).

Table 1 Performance comparison with different values of the embedding coefficient

Images	Attack	$\alpha = 0.01$		$\alpha = 0.05$		$\alpha = 0.1$		$\alpha = 0.2$		$\alpha = 0.3$	
		PSNR	SSIM	PSNR	SSIM	PSNR	SSIM	PSNR	SSIM	PSNR	SSIM
Gold-hill	None	51.32	0.8705	46.36	0.9857	43.00	0.9850	39.36	0.9743	37.28	0.9522
	Cropping 1/4	11.14	-0.1635	11.14	0.7439	11.13	0.8120	11.11	0.8211	11.08	0.8007
	Histogram equalization	16.54	0.4114	16.53	0.6114	16.48	0.7223	16.31	0.8085	16.15	0.8409
	Median filtering 3x3	33.34	-0.1543	33.03	0.7025	32.29	0.8325	30.81	0.8813	29.66	0.8811
	Speckle noise 2%	24.31	0.2307	24.24	0.3721	24.08	0.5373	23.58	0.7410	23.07	0.8113
	Gaussian noise $\mu=0$, $v=0.005$	23.15	0.1987	23.10	0.3158	22.99	0.4500	22.60	0.6598	22.19	0.7526
	Salt & pepper noise 2%	21.98	0.1978	21.97	0.2953	21.82	0.4149	21.66	0.6075	21.28	0.7226
Air-plane	None	51.28	0.8771	46.54	0.9931	43.54	0.9546	39.99	0.8800	38.03	0.8004
	Cropping 1/4	8.70	-0.0344	8.70	0.6020	8.70	0.6990	8.69	0.6831	8.68	0.6121
	Histogram equalization	11.25	0.3121	11.25	0.4496	11.23	0.5464	11.20	0.5891	11.19	0.5922
	Median filtering 3x3	34.26	-0.1669	33.76	0.6722	32.97	0.8008	31.56	0.8206	30.55	0.7739
	Speckle noise 2%	19.81	0.1765	19.79	0.2504	19.75	0.3313	19.60	0.4688	19.44	0.5386
	Gaussian noise $\mu=0$, $v=0.005$	23.04	0.1777	22.99	0.3116	22.89	0.4392	22.59	0.6042	22.30	0.6420
	Salt & pepper noise 2%	21.82	0.1742	21.76	0.2878	21.81	0.4024	21.50	0.5711	21.23	0.6244
House	None	51.29	0.8645	46.31	0.9931	42.92	0.9946	39.45	0.9667	37.53	0.9291
	Cropping 1/4	9.59	-0.0707	9.59	0.8396	9.58	0.9513	9.57	0.9528	9.55	0.9212
	Histogram equalization	19.79	0.3177	19.74	0.4863	19.68	0.5751	19.60	0.6814	19.45	0.7348
	Median filtering 3x3	42.78	-0.1691	41.33	0.6467	39.38	0.8606	36.86	0.8998	35.20	0.8784
	Speckle noise 2%	21.83	0.2123	21.80	0.3046	21.69	0.4155	21.45	0.5999	21.16	0.6900
	Gaussian noise $\mu=0$, $v=0.005$	23.03	0.1996	22.99	0.3215	22.86	0.4621	22.52	0.6401	22.17	0.7381
	Salt & pepper noise 2%	22.34	0.2055	22.23	0.2966	22.19	0.4248	21.92	0.6127	21.58	0.7100



Fig. 7. Stego Goldhill image subjected to different attacks with the extracted secret Peppers image of each one: (a) Original cover and secret images, (b) Stego and extracted secret images with no attack, (c) Cropping 1/4, (d) Histogram equalization, (e) Median filtering 3x3, (f) Speckle noise (1%), (g) Gaussian noise ($\mu = 0, v = 0.002$), (h) Salt & pepper noise (1%)

Table 2 Quality performance comparison

Images	Attack	Scheme in [19]		Proposed scheme	
		PSNR	SSIM	PSNR	SSIM
Goldhill	Cropping 1/4	11.12	0.7754	11.13	0.8120
	Histogram equalization	16.31	0.7715	16.48	0.7223
	Median filtering 3x3	32.48	0.1944	32.29	0.8325
	Speckle noise 1%	25.89	0.4902	26.74	0.6630
	Gaussian noise $\mu=0, v=0.002$	25.81	0.4413	26.61	0.6209
	Salt & pepper noise 1%	24.12	0.3700	24.71	0.5323
Airplane	Cropping 1/4	8.69	0.7297	8.70	0.6990
	Histogram equalization	11.18	0.4445	11.23	0.5464
	Median filtering 3x3	33.07	0.0681	32.97	0.8008
	Speckle noise 1%	22.32	0.2878	22.57	0.4160
	Gaussian noise $\mu=0, v=0.002$	26.08	0.4121	26.63	0.6119
	Salt & pepper noise 1%	24.17	0.3461	24.60	0.5312
House	Cropping 1/4	9.57	0.8605	9.58	0.9513
	Histogram equalization	19.48	0.6451	19.68	0.5751
	Median filtering 3x3	40.00	0.0716	39.38	0.8606
	Speckle noise 1%	23.84	0.3624	24.41	0.5195
	Gaussian noise $\mu=0, v=0.002$	25.66	0.4240	26.55	0.6313
	Salt & pepper noise 1%	24.28	0.3659	25.09	0.5473

In order to show the advantage of using YCbCr space in this work, table 3 presents a comparative analysis of the proposed algorithm with RGB color space by using PSNR and

SSIM. According to SSIM values in table 3, the proposed algorithm has better performance in secret image extraction when using YCbCr compared with RGB space.

Table 3 Performance comparison between RGB and YCbCr spaces

Image	Attack	RGB – red component		RGB – green component		RGB – blue component		Proposed YCbCr	
		PSNR	SSIM	PSNR	SSIM	PSNR	SSIM	PSNR	SSIM
Goldhill	Cropping 1/4	11.14	0.0660	11.14	0.3049	11.14	0.3167	11.13	0.8120
	Histogram equalization	16.54	0.4808	16.55	0.5119	16.54	0.4993	16.48	0.7223
	Median filtering 3x3	33.20	0.1162	33.06	0.2466	33.10	0.2263	32.29	0.8325
	Speckle noise 1%	27.06	0.6261	27.06	0.5739	27.06	0.6231	26.74	0.6630
	Gaussian noise $\mu=0, v=0.002$	26.91	0.6189	26.90	0.5902	26.90	0.5896	26.61	0.6209
	Salt & pepper noise 1%	24.98	0.5289	24.89	0.4689	24.89	0.4665	24.71	0.5323
Airplane	Cropping 1/4	8.70	0.2672	8.70	0.0338	8.70	0.2612	8.70	0.6990
	Histogram equalization	11.26	0.4208	11.25	0.3882	11.25	0.3983	11.23	0.5464
	Median filtering 3x3	33.95	0.3086	34.01	0.1281	34.01	0.2983	32.97	0.8008
	Speckle noise 1%	22.65	0.3621	22.67	0.3495	22.66	0.3323	22.57	0.4160
	Gaussian noise $\mu=0, v=0.002$	26.87	0.5644	26.89	0.5405	26.90	0.5163	26.63	0.6119
	Salt & pepper noise 1%	24.79	0.4554	24.83	0.4572	24.94	0.4281	24.60	0.5312
House	Cropping 1/4	9.59	0.6087	9.59	0.3502	9.59	0.3533	9.58	0.9513
	Histogram equalization	19.68	0.5279	19.75	0.5075	19.76	0.4807	19.68	0.5751
	Median filtering 3x3	41.10	0.7711	41.28	0.7877	41.73	0.5543	39.38	0.8606
	Speckle noise 1%	24.60	0.3749	24.61	0.3946	24.60	0.3917	24.41	0.5195
	Gaussian noise $\mu=0, v=0.002$	26.87	0.4818	26.88	0.4821	26.88	0.5002	26.55	0.6313
	Salt & pepper noise 1%	25.29	0.4288	25.26	0.4034	25.25	0.4135	25.09	0.5473

7. Conclusions

In this work, a color image steganography method for hiding secret information is presented. The secret information, which can be a grayscale image or even a text that has been converted into an image, is encoded into DWT coefficients of vertical sub-band HL2 of YCbCr cover image based on SVD technique. The key feature of the proposed scheme is the use of three transformation techniques (YCbCr space, DWT, and (SVD) which provides a higher level of imperceptibility. Furthermore, the proposed method provides an acceptable tradeoff between robustness and perceptual quality, which is controlled by the value of embedding coefficient α according to the characteristics of the cover image and the desired robustness level. The advantage of using YCbCr space over RGB is that the high decorrelation of its color components that provides better robustness against attacks as well as the perceptual quality of images. Experimental results and simulations demonstrate that the proposed method achieves both imperceptibility and robustness even when the stego image is exposed to various attacks.

References

- [1] X. Duan, D. Guo, N. Liu, B. Li, M. Gou and C. Qin, A New High Capacity Image Steganography Method Combined With Image Elliptic Curve Cryptography and Deep Neural Network, in *IEEE Access*, vol. 8, 2020, pp. 25777-25788.
- [2] M. Khari, A. K. Garg, A. H. Gandomi, R. Gupta, R. Patan and B. Balusamy, Securing Data in Internet of Things (IoT) Using Cryptography and Steganography Techniques, in *IEEE Transactions on Systems, Man, and Cybernetics: Systems*, vol. 50, no. 1, Jan. 2020, pp. 73-80.
- [3] Ghazwan Jabbar Ahmed, Adel Jalal Yousif and Fadhil Kadhim Zaidan, A Digital Image Watermarking Scheme based on Discrete Cosine Transform, *Journal of Engineering and Applied Sciences*, Volume 14, Issue 16, 2019, pp 5762-5768.
- [4] D. N. Aini, D. R. I. Moses Setiadi, S. N. Putro, E. H. Rachmawanto and C. A. Sari, Survey of Methods in the Spatial Domain Image Steganography based Imperceptibility and Payload Capacity, 2019 International Seminar on Application for Technology of Information and Communication (iSemantic), Semarang, Indonesia, 2019, pp. 434-439.
- [5] Ashty M. Aaref, Video Steganography Using LSB Substitution and Sobel Edge Detection, *Diyala Journal of Engineering Sciences*, Vol. 11, No. 2, June 2018, pp. 67-73.
- [6] T. Taburet, P. Bas, J. Fridrich and W. Sawaya, Computing dependencies between DCT coefficients for natural steganography in JPEG domain, *Proc. ACM Workshop Inf. Hiding Multimedia Secur.*, Jul. 2019, pp. 57-62.
- [7] S. Al-Azawi, A. Abedelkareem, Low complexity multilevel 2-D DHWT architecture. The second engineering scientific conference-college of engineering, Diyala University. *Diyala Journal of Engineering Sciences*. 8(4), 2015, pp. 493–500.
- [8] Kadhim, I.J., Premaratne, P., Vial, P.J., Halloran, B. Comprehensive survey of image steganography, techniques, Evaluations, and trends in future research. *Neurocomputing* 335 (2019), pp. 299–326.
- [9] S.S. Baawi, M.R. Mokhtar, R. Sulaiman, A comparative study on the advancement of text steganography techniques in digital media, *ARPN J. Eng. Appl. Sci.* 13 (2018), pp. 1854–1863
- [10] A. Girdhar and V. Kumar, Comprehensive survey of 3D image steganography techniques, in *IET Image Processing*, vol. 12, no. 1, 2018, pp. 1-10.
- [11] M. Parul and R. Harish, Optimized Image Steganography Using Discrete Wavelet Transform (DWT), *International Journal of Recent Development in Engineering and Technology*, vol. 2, no. 2, , 2014, pp. 75–81.
- [12] T. Narasimmalou and Allen Joseph. R, Optimized Discrete Wavelet Transform Based Steganography, *IEEE International Conference on Advance Communication Control and Computing Technologies (ICACCCT)*, 2012, pp. 88-91.
- [13] Y. Chen, Z. Jia, Y. Peng and Y. Peng, Robust Dual-Color Watermarking Based on Quaternion Singular Value Decomposition, in *IEEE Access*, vol. 8, 2020, pp. 30628-30642.
- [14] Rajaa aldeen Abad Khalid , Aman Ala'a Hussain, Multi-level Steganography System Using Wavelet Transform, *Journal of Engineering and Sustainable Development*, Vol. 22, No. 03, May 2018, pp. 50-61.
- [15] Kaiser J. Giri , Mushtaq Ahmad Peer and P. Nagabhushan, A Robust Color Image Watermarking Scheme Using Discrete Wavelet

Transformation, I.J. Image, Graphics and Signal Processing, 2015, pp. 47-52.

- [16] Adel Jalal Yousif, A Discrete Cosine Transform Based Watermarking Scheme For Color Image Using Ycbr Space, Journal of Engineering and Sustainable Development Vol. 22, No.06, November 2018, pp. 1-12.
- [17] Y. Shahriari, R. Fidler, M. M. Pelter, Y. Bai, A. Villaroman and X. Hu, Electrocardiogram Signal Quality Assessment Based on Structural Image Similarity Metric, in IEEE Transactions on Biomedical Engineering, vol. 65, no. 4, April 2018, pp. 745-753.
- [18] Muna M. Jawad, Ekbal H. Ali, and Adel J. Yousif, A Fuzzy Random Impulse Noise Detection and Reduction Method Based on Noise Density Estimation, International Journal of Scientific & Engineering Research, Volume 5, Issue 3, March-2014, pp. 455-468.
- [19] M. Douglas, K. Bailey, and M. Leeney, K. Curran, Using SVD and DWT Based Steganography to Enhance the Security of WatermarkedFingerprint Images,Telkonnika, vol. 15, No. 3, Sep. 2017, pp. 1368-1379.